

EXPERIMENTAL STUDY

Hsa_circ_0097009 regulates proliferation, apoptosis, migration and invasion of hepatocellular carcinoma cells via miR-568/RNF38 axis

Ziliang WU*, Huakang LI*, Wei LIU, Rongkai HUANG, Bing LIN

Health Management Center, Hospital of Chengdu University of Traditional Chinese Medicine, Jinniu District, Chengdu, China. L1284516264@163.com

ABSTRACT

BACKGROUND: Circular RNAs (circRNAs), a class of non-coding RNAs, has been proved as an essential driver of hepatocellular carcinoma (HCC) progression. However, the aim of this study is to explore the role of hsa_circ_0097009 (circ_0097009) in HCC progression.

METHODS: Ki67 expression in HCC tissues was labeled and examined by IHC assay. Quantitative real-time PCR (qRT-PCR) was applied to assess the expression of circ_0097009, miR-568 and RING finger protein 38 (RNF38). Western blot assay was conducted to analyze protein expression. HCC cell colony formation, proliferation, migration, invasion, angiogenesis ability and apoptosis were determined by colony formation assay, 5-ethynyl-29-deoxyuridine (EdU) assay, wound healing assay, trans well assay, angiogenesis assay and flow cytometry. The interaction between circ_0097009 and miR-568 as well as miR-568 and RNF38 was probed by dual-luciferase reporter and RNA immunoprecipitation (RIP) assays.

RESULTS: We found that circ_0097009 and RNF38 expressions were markedly higher, but miR-568 expression was significantly lower in HCC. Circ_0097009 knockdown blocked HCC cell cloning, proliferation, migration, invasion, angiogenesis and facilitated apoptosis. MiR-568 was a target of circ_0097009 in HCC cells. MiR-568 interference could attenuate the circ_0097009 knockdown-induced inhibition on HCC cells progress. MiR-568 depressed cell clonal formation, proliferation, migration, invasion, angiogenesis and promotion of apoptosis, by targeting RNF38, and RNF38 overexpression reversed the suppression of miR-568 in HCC cells. Also, circ_0097009 knockdown blocked tumor growth *in vivo*.

CONCLUSION: Together, this study indicated that the oncogenic function of circ_0097009 in HCC, and circ_0097009/miR-568/RNF38 axis was expected to be a novel therapeutic option for HCC patients (Tab. 1, Fig. 7, Ref. 33). Text in PDF www.elis.sk

KEY WORDS: circ_0097009, miR-568, RNF38, hepatocellular carcinoma.

Introduction

Hepatocellular carcinoma (HCC) is the third leading cause of cancer-related death worldwide, after lung cancer and gastric cancer (1). HCC treatment has evolved rapidly, but recurrence rate and prognostic outcome are not promising (2, 3), and 5-year survival rate is discouraging (4, 5). Therefore, it is imperative to dissect HCC internal molecular mechanism, which is expected to contribute to HCC patients' treatment.

Circular RNAs (circRNAs), a type of non-coding RNAs (ncRNAs), are the latest research hotspot for a variety of cancers, including HCC (6–8). The closed-loop structure of circRNAs makes them more stable and conservative (9). With the develop-

ment of high-throughput sequencing technology, a large number of circRNAs have been discovered (10, 11). Previous studies have uncovered the important regulatory roles of circRNAs in HCC progression. Wang et al indicated that hsa_circ_0003141 downregulation repressed UBAP2 expression, inhibited the growth and pro-

Tab. 1. Primer sequences used for qRT-PCR.

Name		Primers (5'-3')
circ_0097009	Forward	TCAAAGGACTCCACTGATGGAT
	Reverse	GTCCCACTGTAAGCACAGGC
miR-568	Forward	GCCGAG ATGTATAAATGTAT
	Reverse	ATCCAGTGCAGGGTCCGAGG
RNF38	Forward	GTGGAACAACAAAGGGGGTTTCG
	Reverse	CTGAATGAGAGAGGGCGCTGT
SLC5A8	Forward	CCTGTTTCGCTTTGGGCATT
	Reverse	ATCCAGCCATCAGACCAACAA
U6	Forward	CTCGCTTCGGCAGCACATA
	Reverse	CGAATTGCGTGTCATCT
GAPDH	Forward	AAGGCTGTGGCAAGGTCATC
	Reverse	GCGTCAAAGGTGGAGGAGTGG

Health Management Center, Hospital of Chengdu University of Traditional Chinese Medicine, Chengdu, China

Address for correspondence: Bing LIN, Health Management Center, Hospital of Chengdu University of Traditional Chinese Medicine, No. 39, Shi-er-giao Road, Chengdu, 610072, Sichuan Province, P. R. China

*These authors contribute equally to this study.

liferation of HCC cells (12). Guo et al reported that circ_0015756 aggravated HCC progression by sponging miR-610 (13). This study aims to reveal the potential mechanism of circ_0097009 in HCC.

MicroRNAs (miRNAs) have been reported to act as tumor suppressors or carcinogenic molecules in HCC cells, regulating HCC occurrence (14). A previous study suggested that miR-26a was considered an antitumor factor that leads to the inhibition of HCC cell proliferation (15). In this study, we explored the interaction between miR-568 and circ_0097009 and further analyzed their functional association in regulating HCC cell behaviors.

Ring finger protein 38 (RNF38), a member of the ubiquitin ligase family with RING domain, was involved in the pathological process of several diseases, including HCC (16–19). Previous studies have claimed that RNF38 could be targeted by miR-7 (20). The interaction between miR-568 and RNF38 has never been reported.

In brief, we evaluated circ_0097009 function in HCC development, both *in vivo* and *in vitro*. In addition, we identified the regulatory mechanisms of the circ_0097009/miR-568/RNF38 axis, and these findings may shed a little light on HCC interaction network.

Materials and methods

Patient samples and cell lines

35 pairs of HCC tissues and normal tissues were acquired from HCC patients treated at the Hospital of Chengdu University of Tra-

ditional Chinese Medicine. Written informed consent was obtained from each patient included in the study and the study protocol conforms to the ethical guidelines of the 1975 Declaration of Helsinki as reflected in a priori approval by the Ethics Committee of Hospital of Chengdu University of Traditional Chinese Medicine.

Human immortalized liver cell lines (THLE-2) and HCC cell lines (Huh7 and SNU-387) were got from the American Type Culture Collection Center (ATCC, Manassas, VA, USA) and cultured in Dulbecco's modified Eagle's medium (DMEM) medium (Gibco, Carlsbad, CA, USA) containing 10% fetal bovine serum (FBS; Gibco) at 37°C with 5% CO₂.

Cell transfection

Small interfering (si)RNA of circ_0097009 (si-circ_0097009), siRNA negative control (si-NC), short hairpin (sh)RNA of circ_0097009 (sh-circ_0097009), shRNA NC (sh-NC), miR-568 mimic, miRNA NC, miR-568 inhibitor, inhibitor NC, RNF38 expressing plasmid in pcDNA vector (pc-RNF38), and pc-NC were purchased by GenePharma (Shanghai, China). Lipofectamine 3000 Reagent (Thermo Fisher Scientific, Waltham, MA, USA) was transfected according to manufacturer's directions.

Immunohistochemistry (IHC) assay

The protein level of Ki67 in xenograft tumor tissues was analyzed by IHC assay using a Histostain-Plus IHC kit (NeoBioscience, Guangzhou, China) according to the operating instructions.

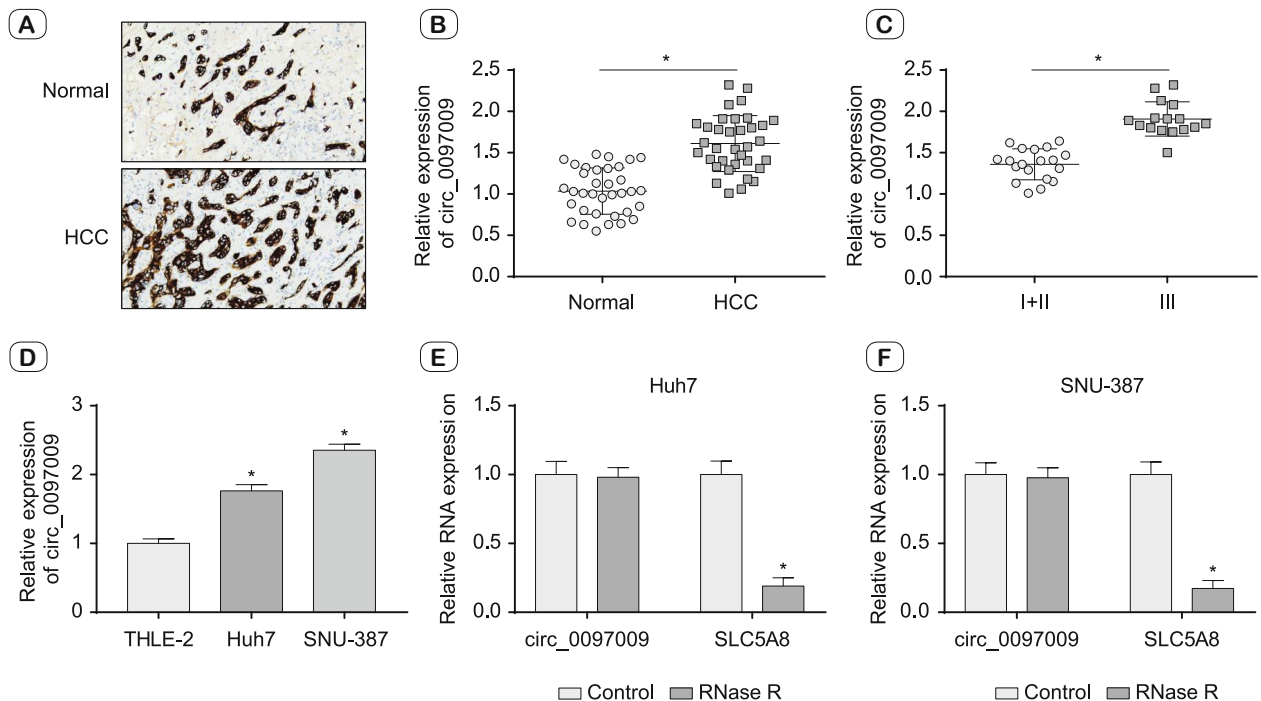


Fig. 1. Circ_0097009 was upregulated in HCC. **A.** Ki67 analysis of HCC tissues and normal tissues. **B.** Relative expression level of circ_0097009 was analyzed by qRT-PCR in HCC tissues (n=35). **C.** Circ_0097009 expression under different staging. **D.** Relative expression level of circ_0097009 in HCC cells (Huh7 and SNU-387). **E, F.** Relative RNA expression of circ_0097009 and SLC5A8 after RNase R treatment. * $p < 0.05$.

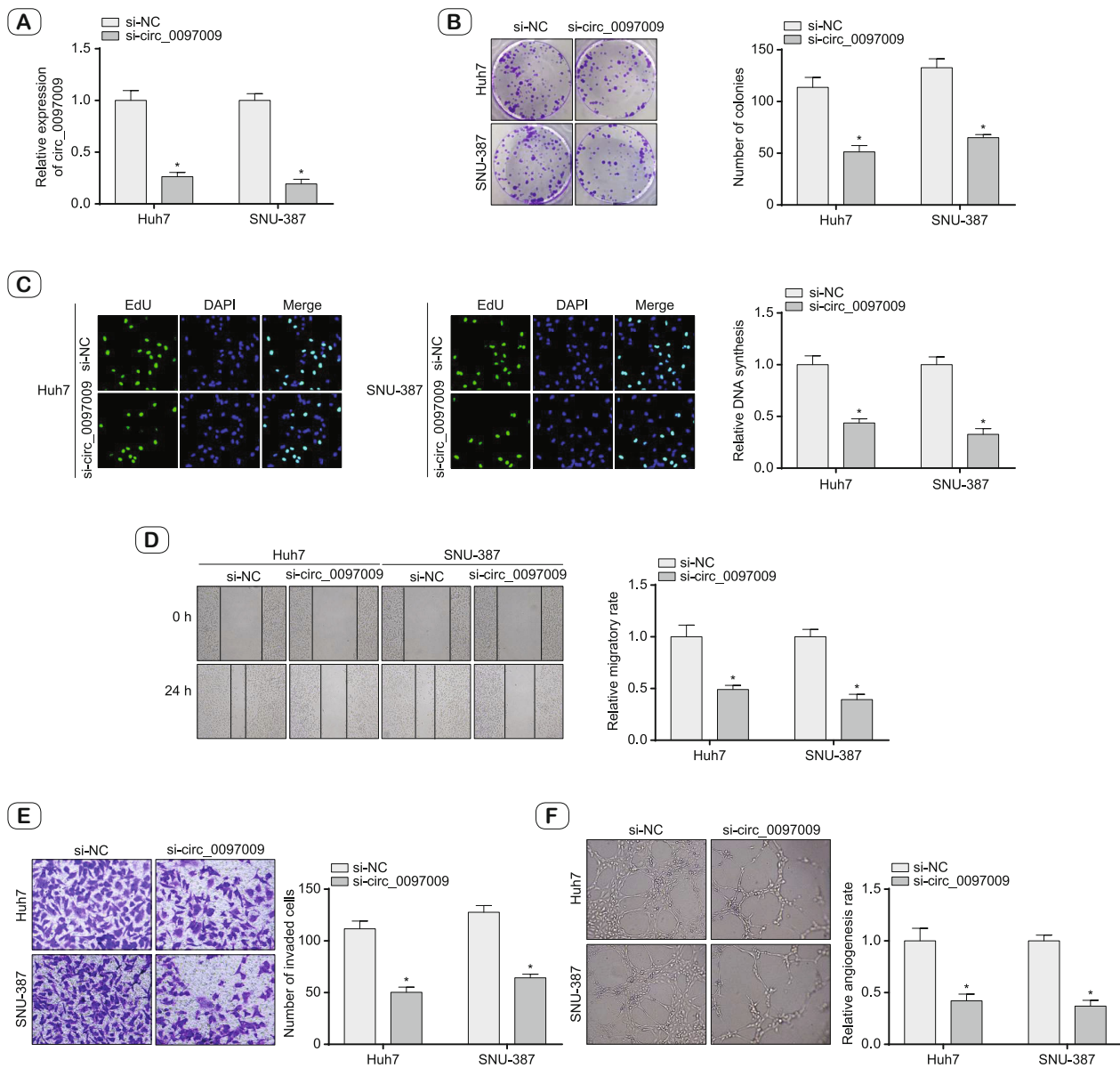


Fig. 2. Depletion of circ_0097009 inhibited HCC progression. HCC cells (Huh7 and SNU-387) were transfected with si-NC or si-circ_0097009. **A.** Relative expression of circ_0097009 in HCC cells. **B.** Colony formation assay for the colony formation ability of HCC cells. **C.** EdU assay for HCC cell proliferation. **D, E.** Transwell assay for number of migrated and invaded cells in HCC cells. **F.** Relative angiogenesis rate of HCC cells. **G.** Flow cytometry for apoptosis rate in HCC cells. **H, I.** Western blot assay for the protein levels of Bax and Bcl-2 in HCC cells. * $p < 0.05$.

Western blot assay

Cells were disrupted with cell lysis buffer (Beyotime, Shanghai, China). Protein samples were boiled and were loaded onto sodium dodecyl sulfate polyacrylamide gel electrophoresis (SDS-PAGE). Subsequently, the protein bands were transferred onto the polyvinylidene fluoride (PVDF) membrane. The membrane was blocked with 5% skimmed milk and was incubated with the primary antibodies overnight, including anti-B cell leukemia/lymphoma 2 (anti-Bcl-2; AF6139; 1:5000; affinity), anti-Bcl-2

associated X, apoptosis regulator (anti-Bax; AF0120; 1: 8000; affinity, Jiangsu, China), anti-RNF38 (PA5-42335; 1: 3000; Thermo Fisher Scientific), and anti-glyceraldehyde-3-phosphate dehydrogenase (anti-GAPDH; MA5-15738-D680; 1: 20000; Thermo Fisher Scientific). The next day, the membrane was incubated with the secondary antibody (Thermo Fisher Scientific) for 2 h.

The protein signals were visualized using an enhanced chemiluminescence (ECL)-PLUS/Kit (GE Healthcare, Piscataway, NJ, USA).

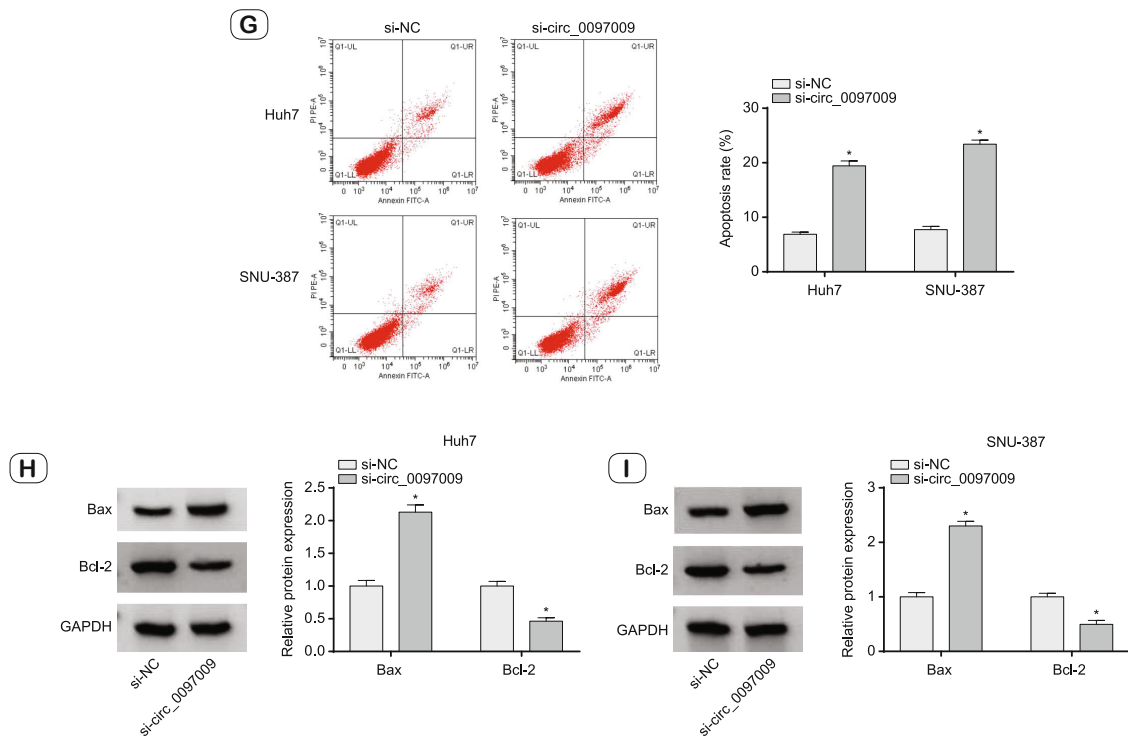


Fig. 2.

Quantitative real-time polymerase chain reaction (qRT-PCR) and RNase R digestion

Total RNA was derived from HCC samples using TRIzol reagent (Beyotime). Reverse transcription was conducted using PrimeScript RT Reagent Kit (Takara, Dalian, China) or a miScript Reverse Transcription Kit (Qiagen, Valencia, CA, USA). QRT-PCR was performed using PrimeScript RT kit (Takara) and SYBR Master Mix (Applied Biosystems, Foster City, USA) while the data were calculated with $2^{-\Delta\Delta Ct}$ method. MiRNA expression was normalized to U6, while the expression of circRNA and mRNA was normalized to GAPDH. To assess circ_0097009 stability, RNA was randomly divided into 2 groups. The experimental group was added with RNase R (Applied Biological Materials, Vancouver, Canada) and incubated for 20 min at 37 °C, and un-treated group acted as the control. Then circ_0097009 expression was determined. All primer sequences are shown in Table 1.

Colony formation assay

Transfected Huh7 and SNU-387 cells (1000 cells/well) were seeded on 6-well plates and cultured for 14 days. HCC cells were fixed with methanol (EpiZyme, Shanghai, China) and colored with crystal violet (EpiZyme). Under the microscope (Olympus, Tokyo, Japan), the colonies larger than 100 μm in diameter were captured and counted by Image J.

EdU assay

EdU method was assayed for HCC cell proliferative capacity. HCC cells (1×10^5) were cultured in 96-well plates. After the

culture was completed, half of the medium was replaced with 20 μM EdU solution. HCC cells were incubated for 12 h in darkness, then the medium was removed, HCC cells were fixed and permeated, and finally EdU detection was performed.

Wound healing assay and transwell assay

Regarding wound healing assay, transfected HCC cells (5×10^5) were spread in 6-well plates, grown overnight, and scribed vertically. Cells were washed and cell images were taken at 0 h and 24 h.

For invasion assay, Huh7 and SNU-387 cells (1×10^5) in serum-free culture medium were moved to the upper chamber (Corning, Tewksbury, MA, USA), DMEM medium (600 μL , containing 10 % FBS) was added to the lower chamber, incubated at 37 °C for 48 h. Cells penetrating the polycarbonate membrane were fixed with 4 % paraformaldehyde (EpiZyme) for 20 min and stained with 0.5 % crystal violet (EpiZyme) for 15 min. The number of invaded cells was counted under a microscope (Olympus, Tokyo, Japan).

Flow cytometry (FCM)

HCC apoptosis rate was calculated by FCM. Annexin V-fluorescein isothiocyanate (FITC) apoptosis kit (Thermo Fisher Scientific) was applied. After transfection for 72 h, apoptotic HCC cells were assessed using FCM after staining with Annexin V-FITC and propidium iodide (PI) in the dark at indoor temperature for 20 min.

Dual-luciferase reporter assay

Target miRNAs of circ_0097009 and target genes of miR-568 were forecasted by CircInteractome and Starbase. Wild sequences

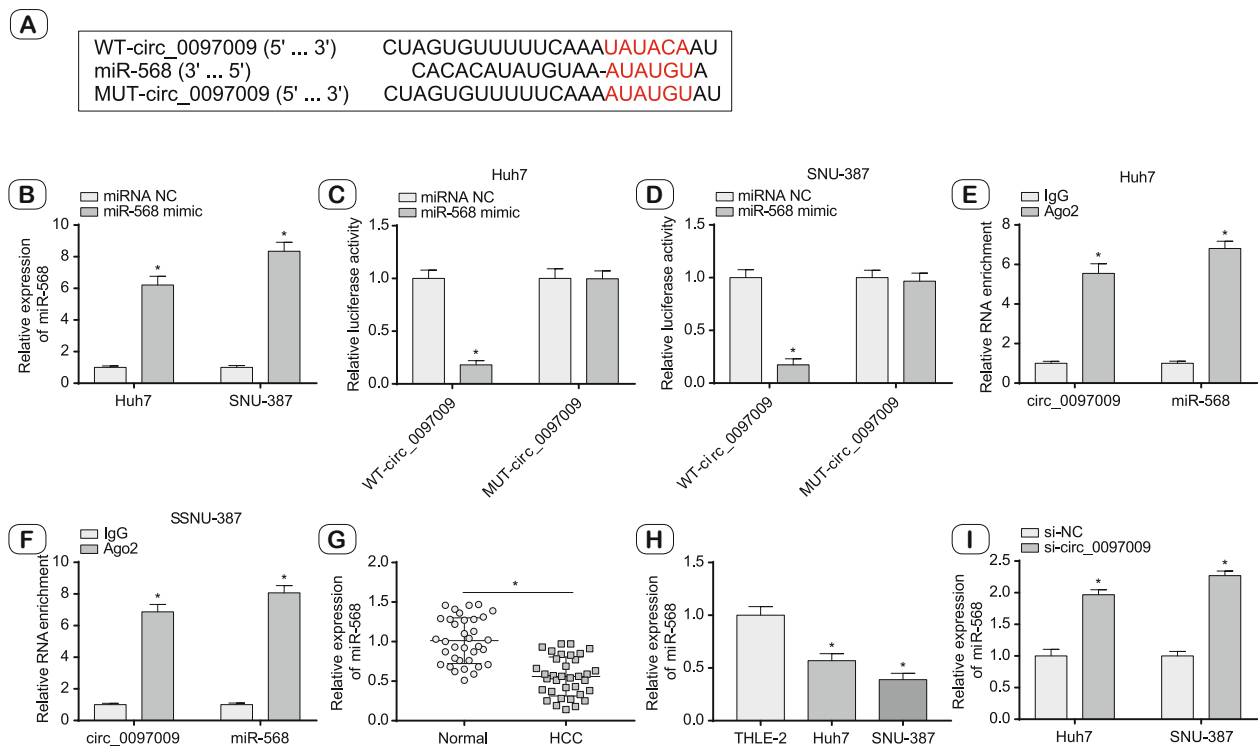


Fig. 3. MiR-568 was a target of circ_0097009. A. CircInteractome was utilized to predict the target miRNAs of circ_0097009. B. Relative expression of miR-568 in HCC cells treated with miRNA NC and miR-568 mimic using qRT-PCR. C, D. Luciferase activity of HCC cells co-transfected with WT-circ_0097009 or MUT-circ_0097009 and miRNA NC or miR-568 mimic were determined. E, F. Relative RNA enrichment of circ_0097009 and miR-568 by RIP assay. G, H. Relative expression level of miR-568 was performed in HCC tissues and cells. I. Relative expression level of miR-568 in HCC cells transfected si-circ_0097009. * $p < 0.05$.

and mutant sequences of circ_0097009 or RNF38-3'UTR were inserted into pmirGLO expression vectors (Promega, Madison, WI, USA), namely WT-circ_0097009 and MUT-circ_0097009, WT-RNF38-3'UTR and MUT-RNF38-3'UTR. After that, the recombinant plasmid with miR-568 mimic or miRNA NC were co-transfected into HCC cells, and dual-luciferase reporter system (Promega) was applied to detect luciferase activity.

RIP assay

The Magna RIP kit (Sigma, St. Louis, MO, USA) was utilized and IgG was taken as the negative control in this study. Transfected Huh7 and SNU-387 cells (1×10^7) were lysed and incubated with anti-Ago2 or anti-IgG magnetic beads for 4 h. RNA enrichment in precipitated complex was analyzed by qRT-PCR.

Tumor-forming analysis in vivo

Our research was approved by the Animal Welfare and Research Ethics Committee of Hospital of Chengdu University of Traditional Chinese Medicine. All animal experiments complied with the ARRIVE guidelines and were carried out in accordance with the National Institutes of Health guide for the care and use of Laboratory animals (NIH Publications No. 8023, revised 1978). SNU-387 cells were transfected with lentivirus vector carrying sh-circ_0097009 or negative control (sh-NC). 6-week-old male

BALB/c nude mice were obtained from Beijing Laboratory Animal Center (Beijing, China). Mice were randomly assigned and injected with SNU-387 cells (5×10^6 cells), subcutaneously. HCC tumor volume was monitored every 7 days. Four weeks later, mice were euthanized and HCC tumors were collected and weighed. Finally, the expressions of circ_0097009, miR-568 and RNF38 were monitored by qRT-PCR and western blot.

Statistical analysis

SPSS software 24.0 (Chicago, IL, USA) was employed for collation analysis. Data were computed using the mean \pm standard deviation (SD) of at least 3 independent trials. Student's *t*-test or one-way analysis of variance (ANOVA) followed by Tukey's test was used to compare the differences in two groups or multiple groups. $P < 0.05$ was considered as significant difference.

Ethics approval and consent to participate

This study complied with Helsinki Declaration and passed the review of the Ethics Committee of Hospital of Chengdu University of Traditional Chinese Medicine.

Our research was approved by the Animal Welfare and Research Ethics Committee of Hospital of Chengdu University of Traditional Chinese Medicine.

Results

Circ_0097009 was expressed at high levels in HCC tissues and cells

We first marked Ki67 in normal tissues and HCC tissues across IHC assay and found the expression level of Ki67 in HCC tissues was higher than in normal tissues (Fig. 1A). Next, we found that *circ_0097009* was expressed at high levels in HCC tissues (n = 35) (Fig. 1B). *Circ_0097009* expression level in stage III (n=16) was obviously higher than that in stage II (n = 19) (Fig. 1C). *Circ_0097009* expression was higher in HCC cells (Huh7 and SNU-387) than in THLE-2 cells (Fig. 1D). In addition, RNase R assay was performed, and our data suggested that *circ_0097009* had a greater stability than linear solute carrier family 5 mem-

ber 8 (SLC5A8) in HCC cells (Figs 1E and 1F). The abnormal up-regulation of *circ_0097009* might imply its important role in HCC progression.

Depletion of circ_0097009 impeded HCC cell proliferation and metastasis

To evaluate the potential role of *circ_0097009* in HCC cells, we knocked down *circ_0097009* expression by RNA interference, and *circ_0097009* expression was greatly declined in HCC cells with si-*circ_0097009* (Fig. 2A). Then, loss-of-function assays about *circ_0097009* were carried out in HCC cells. As seen in Figures 2B and 2C, both the number of colonies and cell proliferation capacity of HCC cells were all notably downregulated upon *circ_0097009* knockdown. Knockdown of *circ_0097009*

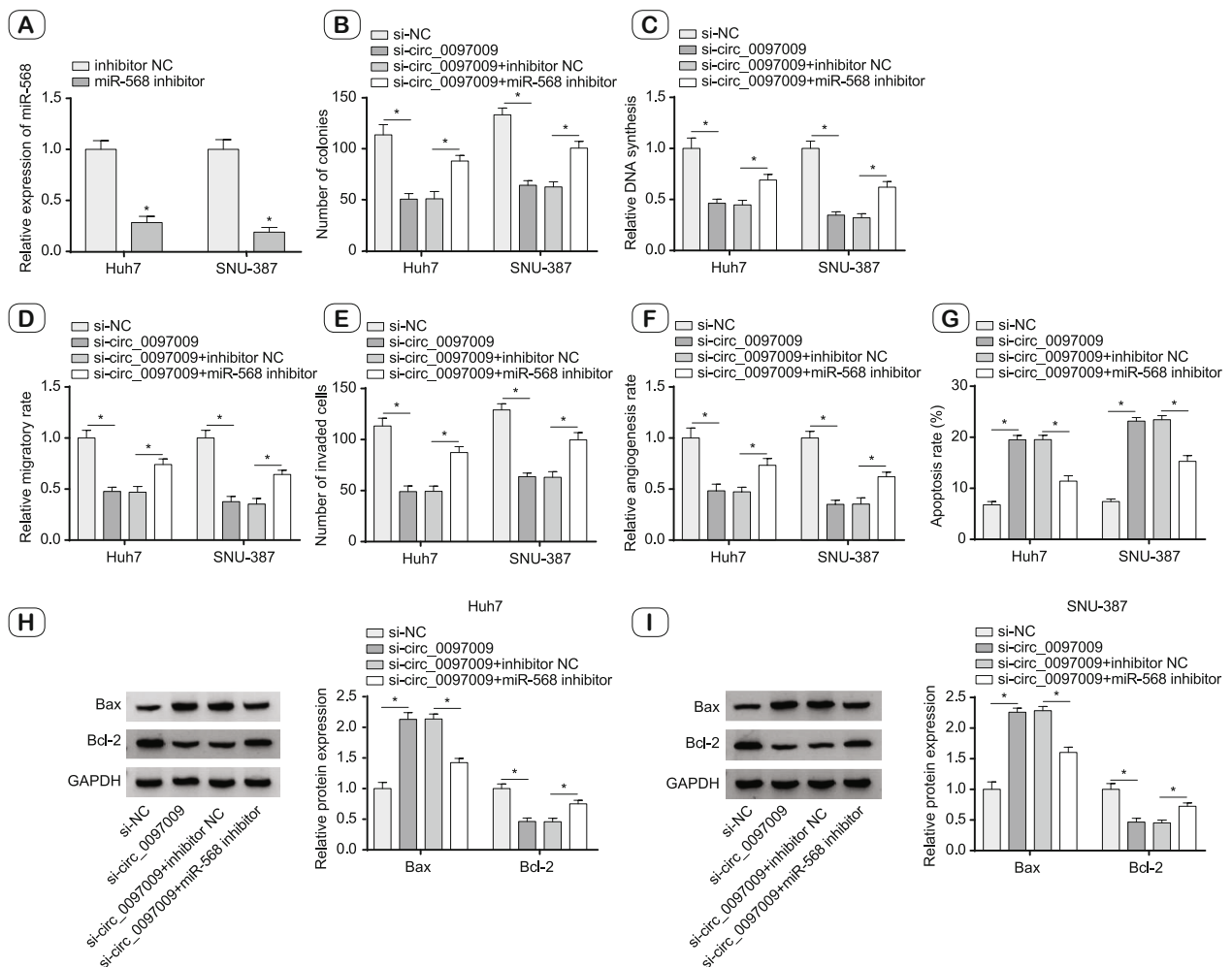


Fig. 4. Interference of miR-568 reversed the *circ_0097009* knockdown-induced inhibition of HCC progression. HCC cells (Huh7 and SNU-387) were transfected with si-NC, si-*circ_0097009*, si-*circ_0097009*+inhibitor NC or si-*circ_0097009*+miR-568 inhibitor. **A.** Relative expression level of miR-568 was performed in HCC cells transfected with miR-568 mimic. **B.** Colony formation assay for the colony formation ability of HCC cells. **C.** EdU assay for HCC cell proliferation. **D, E.** Transwell assay for number of migrated and invaded cells in HCC cells. **F.** Relative angiogenesis rate of HCC cells. **G.** Flow cytometry for apoptosis rate in HCC cells. **H, I.** Western blot assay for the protein levels of Bax and Bcl-2 in HCC cells. * $p < 0.05$.

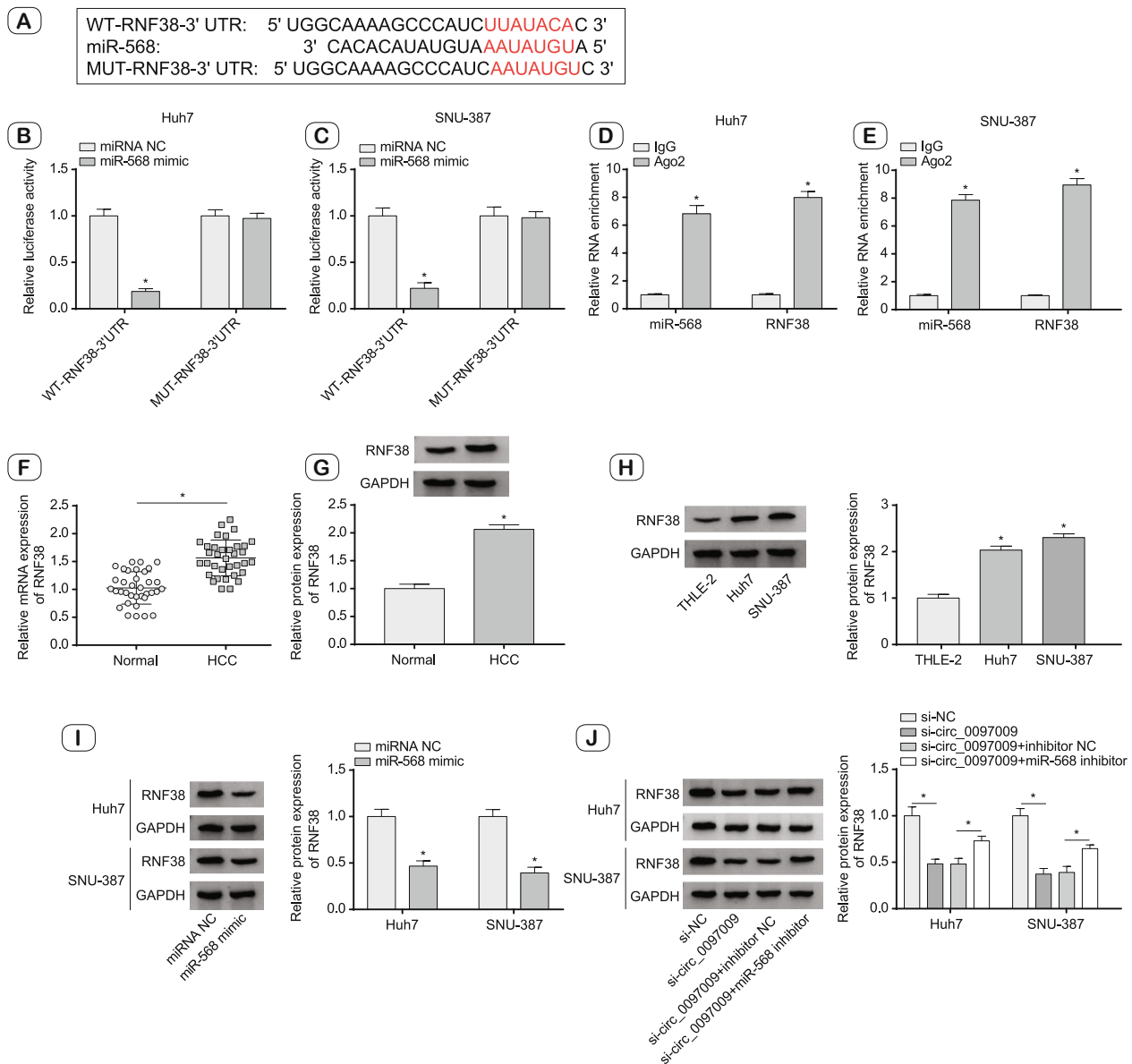


Fig. 5. RNF38 was a target gene of circ_0097009. **A.** Starbase was utilized to predict the target genes of miR-568. **B, C.** Luciferase activity of HCC cells co-transfected with WT-RNF38-3'UTR or MUT-RNF38-3'UTR and miRNA NC or miR-568 mimic were determined. **D, E.** Relative RNA enrichment of miR-568 and RNF38 by RIP assay. **F-H.** Relative expression level of RNF38 was performed in HCC tissues and cells. **I.** Relative expression level of RNF38 in HCC cells transfected with miR-568 mimic. **J.** Relative protein expression of RNF38 in HCC cells under different treatments. * $p < 0.05$.

significantly inhibited HCC cell migration, invasion and angiogenesis rate (Figs 2D–2F). And HCC cell apoptosis rate was elevated by si-circ_0097009 (Fig. 2G). Western blot results verified that circ_0097009 knockdown accelerated Bax expression and restricted Bcl-2 expression (Figs 2H and 2I). These data showed that circ_0097009 knockdown suppressed the proliferation, migration, invasion, and angiogenesis and induced the apoptosis of HCC cells.

Circ_0097009 sponged miR-568 in HCC cells

CircInteractome forecasted that miR-568 has a hypothetical binding site with the circ_0097009 sequence, the binding site was exhibited in Figure 3A. In addition, miR-568 expression was up-regulated by miR-568 mimic in HCC cells (Fig. 3B). Moreover, dual-luciferase reporter assay revealed that HCC cells co-transfected with WT-circ_0097009 and miR-568 mimic had dramatically lower luciferase activity than that in cells co-transfected with

WT-circ_0097009 and miR-NC, yet, luciferase activity of cells co-transfected with MUT-circ_0097009 and miR-NC or miR-568 mimic was changeless (Figs 3C and 3D), showing direct binding of circ_0097009 and miR-568. RIP data further verified that circ_0097009 acted as sponge of miR-568 in HCC cells (Figs 3E and 3F). As depicted in Figures 3G and 3H, miR-568 expression was obviously reduced in HCC tissues and cells compared to corresponding control. And in HCC cells, miR-568 expression was raised by si-circ_0097009 (Fig. 3I). Taken together, miR-568 was a molecular target of circ_0097009 in HCC cells.

The effects of circ_0097009/miR-568 on HCC progression

Then, we carried out rescue experiments about circ_0097009 and miR-568 in HCC cells. We found that miR-568 expression was greatly declined by miR-568 inhibitor (Fig. 4A). As depicted in Figures 4B and 4C, circ_0097009 knockdown apparently decreased the number of colonies and cell proliferation capacity of HCC cells, but miR-568 inhibitor relieved these effects. Wound

healing assay and transwell assay uncovered that miR-568 inhibitor reversed the decreased migration and invasion of HCC cells induced by circ_0097009 knockdown (Figs 4D and 4E). Circ_0097009 knockdown caused the reduction of angiogenesis rate and the elevation of apoptotic rate of HCC cells; these effects were obviously recuperated by miR-568 inhibitor (Figs 4F and 4G). Finally, western blot suggested that si-circ_0097009 resulted in higher Bax expression and lower Bcl-2 expression in HCC cells, and miR-568 inhibitor reversed these impacts (Figs 4H and 4I). These results demonstrated that circ_0097009 knockdown suppressed HCC progression by up-regulating its target miR-568.

MiR-568 aimed to RNF38 in HCC cells

The binding position between RNF38-3'UTR and miR-568 was exhibited in Figure 5A via Starbase prediction. Dual-luciferase reporter assay probed that luciferase activity of HCC cells co-transfected with WT-RNF38-3'UTR and miR-568 was clearly lower than that of cells co-transfected with WT-RNF38-3'UTR

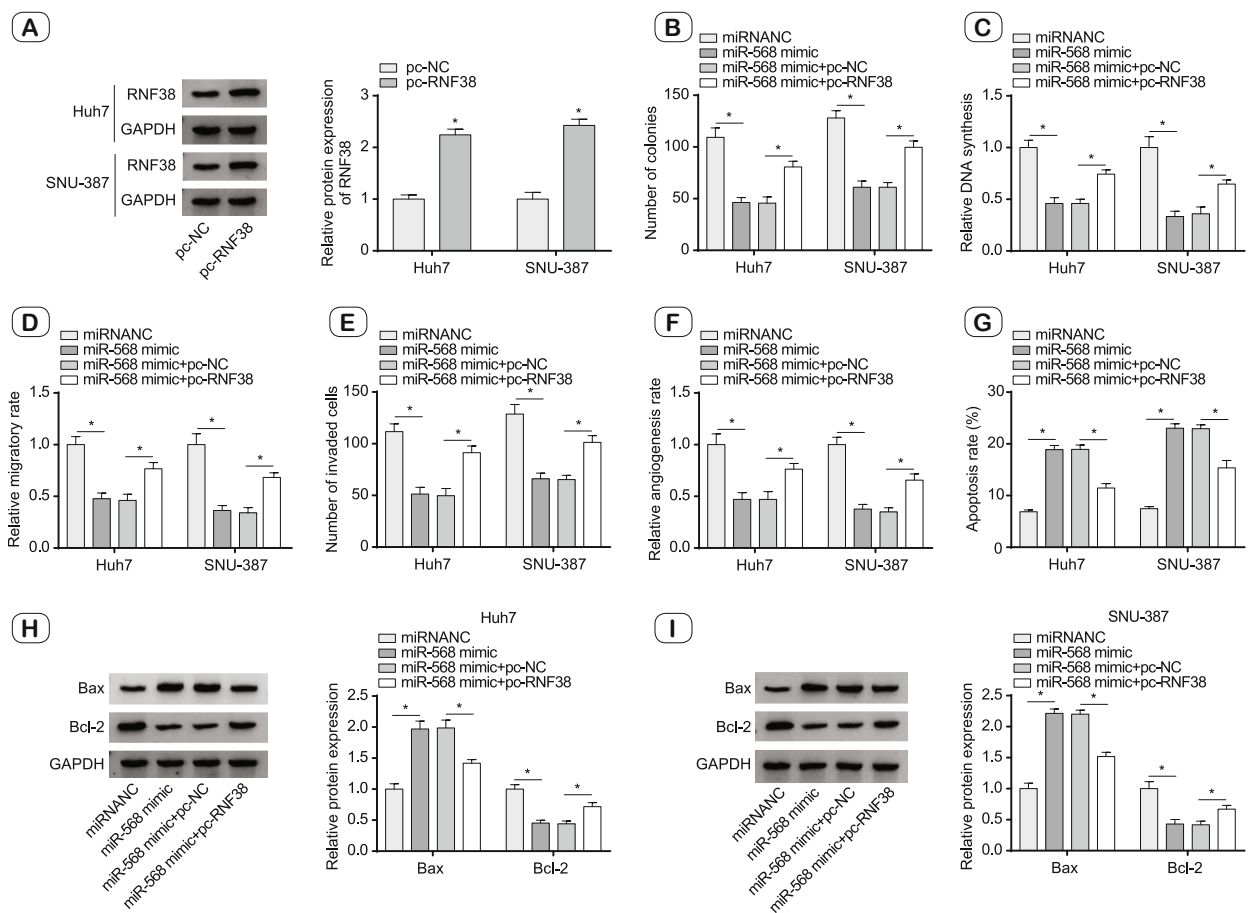


Fig. 6. Interference of RNF38 reversed the miR-568 mimic-induced inhibition of HCC progression. HCC cells (Huh7 and SNU-387) were transfected with miRNA NC, miR-568 mimic, miR-568 mimic+pc-NC or miR-568 mimic+pc-RNF38. A. Relative expression level of RNF38 was performed in HCC cells transfected with pc-RNF38. B. Colony formation assay for the colony formation ability of HCC cells. C. EdU assay for HCC cell proliferation. D, E. Transwell assay for number of migrated and invaded cells in HCC cells. F. Relative angiogenesis rate of HCC cells. G. Flow cytometry for apoptosis rate in HCC cells. H, I. Western blot assay for the protein levels of Bax and Bcl-2 in HCC cells. * $p < 0.05$.

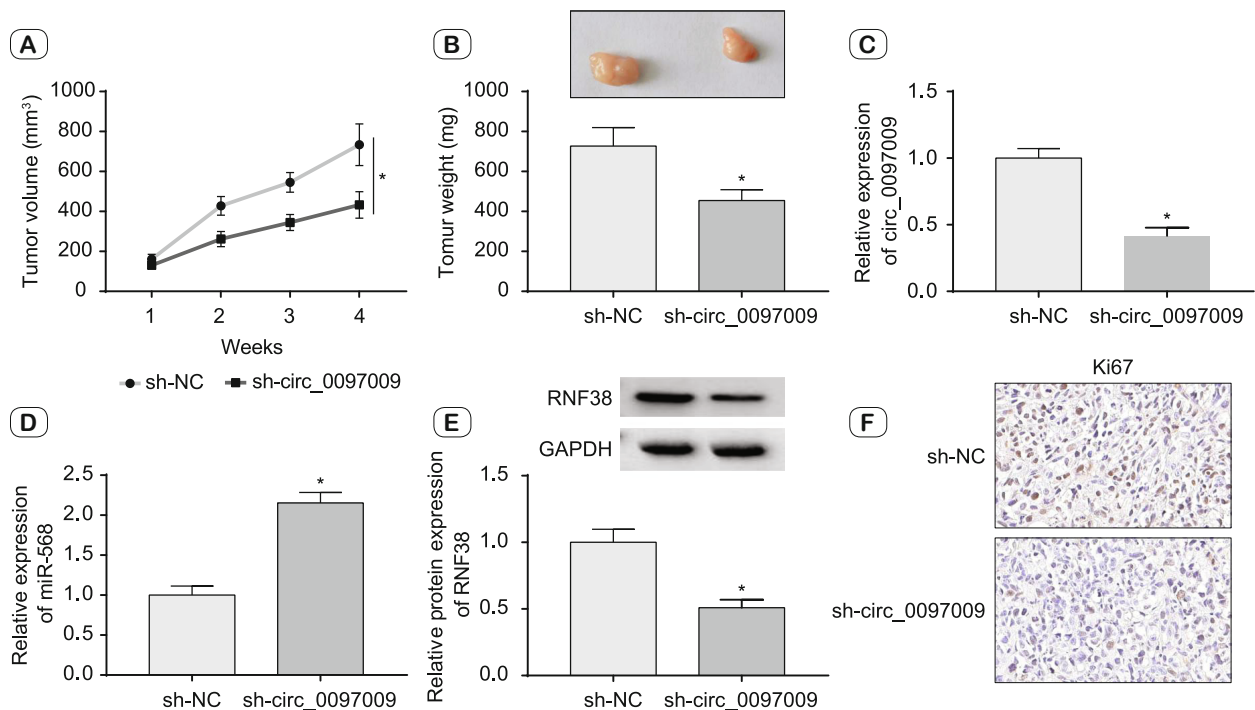


Fig. 7. Knockdown of circ_0097009 suppressed HCC progression in vivo. Nude mice were implanted with HCC cells stably expressing sh-NC or sh-circ_0097009. **A.** Volume of HCC tumor. **B.** Weight of HCC tumor. **C, D.** Relative expression of circ_0097009 and miR-568 in HCC tumor. **E, F.** Relative protein expression of RNF38 and Ki67 in HCC tumor. * $p < 0.05$.

and miRNA NC, while luciferase activity of cells co-transfected with MUT- RNF38-3'UTR and miRNA NC or miR-568 mimic was unchanged (Figs 5B and 5C). Furthermore, RIP assay indicated the direct binding of miR-568 and RNF38 (Figs 5D and 5E). We further surveyed the mRNA and protein expression levels of RNF38, the results suggested that RNF38 expression was higher in HCC tissues and cells in comparison with normal tissues and THLE-2, respectively (Figs 5F–5H). Also, RNF38 protein expression was noticeably repressed by miR-568 in HCC cells (Fig. 5I). As shown in Fig. 5J, RNF38 protein expression was obviously reduced by si-circ_0097009 and was raised by co-transfection si-circ_0097009 with miR-568 inhibitor. Overall, RNF38 was a target of miR-568 in HCC cells.

The effects of miR-568/RNF38 on HCC progression

Next, we analyzed the effects of miR-568/RNF38 in HCC progression. RNF38 protein expression was greatly elevated by RNF38 overexpression (Fig. 6A). MiR-568 mimic weakened number of colonies and cell proliferation capacity, and RNF38 overexpression reversed these impacts (Figs 6B and 6C). What's more, RNF38 overexpression recuperated miR-568-induced down-regulation of migration rate (Fig. 6D), invasion ability (Fig. 6E) and angiogenesis rate (Fig. 6F) in HCC cells. MiR-568 mimic resulted in an increase of apoptotic rate in HCC cells, which were all counteracted by overexpression RNF38 (Fig. 6G). Finally, we performed western blot, and the result suggested that miR-568

mimic resulted in higher Bax expression and lower Bcl-2 expression in HCC cells, while RNF38 overexpression reversed this impact (Figs 6H and 6I). These data revealed that miR-568 overexpression suppressed HCC progression by reducing the expression of its target RNF38.

Circ_0097009 knockdown confined tumorigenesis on HCC in vivo

To further probe circ_0097009 oncogenic role in HCC progression, animal experiments *in vivo* were carried out. SNU-387 cells stably expressing sh-NC or sh-circ_0097009 were inoculated into nude mice, and we tested HCC tumor size weekly and tested HCC tumor weight after 4 weeks. Circ_0097009 silencing greatly impeded HCC tumor volume (Fig. 7A) and weight compared with sh-NC (Fig. 7B). In sh-circ_0097009 group, circ_0097009 expression was downregulated (Fig. 7C) while miR-568 expression was upregulated (Fig. 7D). In addition, the protein expression of RNF38 and Ki67 was suppressed by sh-circ_0097009 (Figs 7E and 7F). Taken together, circ_0097009 knockdown restrained xenograft tumor growth *in vivo*.

Discussion

It is a well-established fact that HCC aggressive characteristic has caused tens of thousands of patients' death (21). Its pathogenesis is tightly linked to circRNAs (22). In HCC, we examined

circ_0097009 aberrant expression and revealed the regulation of the circ_0097009/miR-568/RNF38 axis.

Accumulating evidence have suggested the important regulatory roles of circRNAs in HCC progression (23–26). For instance, Ding *et al* found that circ_0001955 facilitated the proliferation, migration, and invasion abilities of HCC cells by targeting miR-145-5p/NRAS signaling (23). Huang *et al* demonstrated that circ_104348 contributed to HCC progression by targeting miR-187-3p/RTKN2 axis and activating Wnt/ β -catenin signaling (24). However, the role of circ_0097009 in HCC progression remains largely unknown. Here, we found an abnormal increase in circ_0097009 expression in HCC tissues and cells. Regarding functional experiments, the results showed that circ_0097009 knockdown restrained HCC occurrence by blocking colony formation ability, proliferation ability, migration, invasion and promoting apoptosis of HCC cells. Our xenograft assay also illustrated that circ_0097009 interference suppressed tumor growth *in vivo*. These data demonstrated that circ_0097009 played an oncogenic role in HCC development.

CircRNAs can serve as molecular sponges for miRNAs to regulate cell biological behaviors (27, 28). To explore a novel axis of interaction in HCC, we performed functional-recovery experiments and identified miR-568 as a circ_0097009 target, which was confirmed by dual-luciferase reporter assay and RIP assay. A previous study reported that LINC00680 elevated the stemness behaviors and chemo-resistance of HCC cells by sponging miR-568 and up-regulating AKT3 (29), suggesting the tumor suppressor role of miR-568 in HCC. Consistently, we found that miR-568 overexpression restrained the proliferation, migration, invasion, and angiogenesis and facilitated the apoptosis of HCC cells. The data of rescue experiments revealed that circ_0097009 knockdown-induced anti-tumor effects in HCC cells were reversed by silencing miR-568, suggesting that circ_0097009 knockdown suppressed HCC progression by up-regulating the anti-tumor molecule miR-568.

Previous studies have reported that miRNAs can bind to the 3'UTR of mRNAs, thus leading to the degradation or translational suppression of mRNAs (30, 31). We confirmed the interaction between RNF38 and miR-568 in HCC cells. RNF38 has been identified as an oncogene in multiple malignancies (18, 32, 33). For instance, Wu *et al* reported that RNF38 elevated the cisplatin resistance of non-small cell lung cancer cells (33). In HCC, Jia *et al* suggested that RNF38, targeted by miR-7, could reinforce HCC cell proliferation and metastasis (20), suggesting the oncogenic role of RNF38 in HCC. We found that the anti-tumor effects mediated by miR-568 in HCC cells could be largely overturned by the overexpression of RNF38, suggesting that miR-568 hampered HCC development by down-regulating RNF38. The oncogenic role of RNF38 was consistent with the previous study (20). Circ_0097009 could up-regulate RNF38 expression by sponging miR-568 in HCC cells.

Conclusion

We validated the oncogenic role of circ_0097009 in HCC and the molecular mechanism of circ_0097009/miR-568/RNF38 axis.

Circ_0097009 silencing suppressed HCC development by targeting miR-568/RNF38 axis. These findings bestow a hope for HCC patients' treatment.

References

1. Liu J, Li W, Zhang J *et al*. Identification of key genes and long non-coding RNA associated ceRNA networks in hepatocellular carcinoma. *PeerJ* 2019; 7: e8021.
2. Mullath A, Krishna M. Hepatocellular carcinoma – time to take the ticket. *World J Gastrointest Surg* 2019; 11 (6): 287–295.
3. Lu LC, Cheng AL, Poon RT. Recent advances in the prevention of hepatocellular carcinoma recurrence. *Semin Liver Dis* 2014; 34 (4): 427–434.
4. Bruix J, Gores GJ, Mazzaferro V. Hepatocellular carcinoma: clinical frontiers and perspectives. *Gut* 2014; 63 (5): 844–855.
5. Jemal A, Siegel R, Ward E *et al*. Cancer statistics, 2007. *CA Cancer J Clin* 2007; 57 (1): 43–66.
6. Vo JN, Cieslik M, Zhang Y *et al*. The Landscape of Circular RNA in Cancer. *Cell* 2019; 176 (4): 869–881.e813.
7. Klingenberg M, Matsuda A, Diederichs S *et al*. Non-coding RNA in hepatocellular carcinoma: Mechanisms, biomarkers and therapeutic targets. *J Hepatol* 2017; 67 (3): 603–618.
8. Yu J, Xu QG, Wang ZG *et al*. Circular RNA cSMARCA5 inhibits growth and metastasis in hepatocellular carcinoma. *J Hepatol* 2018; 68 (6): 1214–1227.
9. Wilusz JE. A 360° view of circular RNAs: From biogenesis to functions. *Wiley Interdiscip Rev RNA* 2018; 9 (4): e1478.
10. Wu S, Turner KM, Nguyen N *et al*. Circular eCDNA promotes accessible chromatin and high oncogene expression. *Nature* 2019; 575 (7784): 699–703.
11. Kristensen LS, Andersen MS, Stagsted LVW *et al*. The biogenesis, biology and characterization of circular RNAs. *Nat Rev Genet* 2019; 20 (11): 675–691.
12. Wang Y, Gao R, Li J *et al*. Circular RNA hsa_circ_0003141 promotes tumorigenesis of hepatocellular carcinoma via a miR-1827/UBAP2 axis. *Aging (Albany NY)* 2020; 12 (10): 9793–9806.
13. Guo W, Zhao L, Wei G *et al*. Circ_0015756 Aggravates Hepatocellular Carcinoma Development by Regulating FGFR1 via Sponging miR-610. *Cancer Manag Res* 2020; 12: 7383–7394.
14. Hu X, Wang R, Ren Z *et al*. MiR-26b suppresses hepatocellular carcinoma development by negatively regulating ZNRD1 and Wnt/ β -catenin signaling. *Cancer Med* 2019; 8 (17): 7359–7371.
15. Mahati S, Fu X, Ma X *et al*. Delivery of miR-26a Using an Exosomes-Based Nanosystem Inhibited Proliferation of Hepatocellular Carcinoma. *Front Mol Biosci* 2021; 8: 738219.
16. Eisenberg I, Hochner H, Levi T *et al*. Cloning and characterization of a novel human gene RNF38 encoding a conserved putative protein with a RING finger domain. *Biochem Biophys Res Commun* 2002; 294 (5): 1169–1176.
17. Hu PA, Miao YY, Yu S *et al*. Long non-coding RNA SNHG5 promotes human hepatocellular carcinoma progression by regulating miR-363-3p/RNF38 axis. *Eur Rev Med Pharmacol Sci* 2020; 24 (7): 3592–3604.

- 18. Zhang J, Wu H, Yi B et al.** RING finger protein 38 induces gastric cancer cell growth by decreasing the stability of the protein tyrosine phosphatase SHP-1. *FEBS Lett* 2018; 592 (18): 3092–3100.
- 19. Peng R, Zhang PF, Yang X et al.** Overexpression of RNF38 facilitates TGF- β signaling by Ubiquitinating and degrading AHNAK in hepatocellular carcinoma. *J Exp Clin Cancer Res* 2019; 38 (1): 113.
- 20. Jia Y, Li S, Zhang M et al.** Circ_LDLR Knockdown Suppresses Progression of Hepatocellular Carcinoma via Modulating miR-7/RNF38 Axis. *Cancer Manag Res* 2021; 13: 337–349.
- 21. Blum HE.** Molecular therapy and prevention of hepatocellular carcinoma. *Hepatobiliary Pancreat Dis Int* 2003; 2 (1): 11–22.
- 22. Hu J, Li P, Song Y et al.** Progress and prospects of circular RNAs in Hepatocellular carcinoma: Novel insights into their function. *J Cell Physiol* 2018; 233 (6): 4408–4422.
- 23. Ding B, Fan W, Lou W.** hsa_circ_0001955 Enhances In Vitro Proliferation, Migration, and Invasion of HCC Cells through miR-145-5p/NRAS Axis. *Mol Ther Nucleic Acids* 2020; 22: 445–455.
- 24. Huang G, Liang M, Liu H et al.** CircRNA hsa_circRNA_104348 promotes hepatocellular carcinoma progression through modulating miR-187-3p/RTKN2 axis and activating Wnt/ β -catenin pathway. *Cell Death Dis* 2020; 11 (12): 1065.
- 25. Liu Z, Wang Q, Wang X et al.** Circular RNA cIARS regulates ferroptosis in HCC cells through interacting with RNA binding protein ALKBH5. *Cell Death Discov* 2020; 6: 72.
- 26. Wang M, Yang Y, Yang J et al.** circ_KIAA1429 accelerates hepatocellular carcinoma advancement through the mechanism of m(6)A-YTHDF3-Zeb1. *Life Sci* 2020; 257: 118082.
- 27. Hansen TB, Jensen TI, Clausen BH et al.** Natural RNA circles function as efficient microRNA sponges. *Nature* 2013; 495 (7441): 384–388.
- 28. Panda AC.** Circular RNAs Act as miRNA Sponges. *Adv Exp Med Biol* 2018; 1087: 67–79.
- 29. Shu G, Su H, Wang Z et al.** LINC00680 enhances hepatocellular carcinoma stemness behavior and chemoresistance by sponging miR-568 to upregulate AKT3. *J Exp Clin Cancer Res* 2021; 40 (1): 45.
- 30. Fabian MR, Sonenberg N, Filipowicz W.** Regulation of mRNA translation and stability by microRNAs. *Annu Rev Biochem* 2010; 79: 351–379.
- 31. Krol J, Loedige I, Filipowicz W.** The widespread regulation of microRNA biogenesis, function and decay. *Nat Rev Genet* 2010; 11 (9): 597–610.
- 32. Long Y, Zhao Q, Huang Y.** RNF38 enhances 5-Fluorouracil resistance in colorectal cancer by activating the Wnt pathway. *J buon* 2021; 26 (4): 1246–1251.
- 33. Wu C, Chen L, Tao H et al.** RING finger protein 38 induces the drug resistance of cisplatin in non-small-cell lung cancer. *Cell Biol Int* 2021; 45 (2): 287–294.

Received September 26, 2022.

Accepted October 11, 2022.